



ELSEVIER

Deep-Sea Research II 51 (2004) 987–1000

DEEP-SEA RESEARCH
PART II

www.elsevier.com/locate/dsr2

The spring bloom in the northwestern Sargasso Sea: spatial extent and relationship with winter mixing

N.B. Nelson^{a,*}, D.A. Siegel^a, J.A. Yoder^{b,1}

^a*Institute for Computational Earth System Science, University of California at Santa Barbara, Santa Barbara, CA 93106-3060, USA*

^b*Graduate School of Oceanography, University of Rhode Island, Narragansett, RI 02882-1197, USA*

Received 9 December 2002; accepted 19 February 2004

Available online 26 August 2004

Abstract

The interannual variability of the spatial extent of the spring bloom in the central Sargasso Sea was quantified by remote-sensing approaches. Proxy measurements employing satellite-derived sea-surface temperature and chlorophyll *a* concentrations were used to estimate the amount of new production derived from inorganic nitrate supplied by convective winter mixing. Nitrate supply and new productivity were estimated from temperature–nitrate and chlorophyll *a*–euphotic-zone depth relationships derived from in situ measurements made at the US JGOFS Bermuda Atlantic Time-series Study (BATS) site near Bermuda (31°40′ N, 64°10′ W). Proxy estimates of springtime new production at the BATS latitude fall within the range of previous estimates from geochemical approaches, numerical modeling, and analysis of hydrographic measurements. However, estimates of new production made at BATS are poor predictors of the regional-scale new production due to large interannual differences in the spatial gradients of the controlling factors. Moreover, the BATS latitude is in a region of local maxima of meridional gradients in sea-surface temperature and thereby new production. The BATS site lies in a boundary region between the dynamic, spatially variable and productive northern Sargasso Sea and the spring-bloom-free region of the southern Sargasso. Hence, interpretations of spring bloom-forced regional scale biogeochemical processes from point observations made at BATS should be made with caution.

© 2004 Elsevier Ltd. All rights reserved.

1. Introduction

Open-ocean time series have long shown the importance of the variability of biogeochemical processes on seasonal time scales (e.g., Menzel and Ryther, 1961; Longhurst, 1998). However recent studies, such as the US JGOFS time-series stations at Bermuda and Hawaii, have demonstrated the

*Corresponding author. Tel: +1-805-893-3202; fax: +1-805-893-2578.

E-mail address: norm@icess.ucsb.edu (N.B. Nelson).

¹Present address: Division of Ocean Sciences, National Science Foundation, Arlington, VA 22223, USA.

importance of biogeochemical variability on much shorter temporal and spatial scales (Dickey et al., 1993, 1998, 2001; Siegel et al., 1999, 2001, McGillicuddy et al., 1999; Letelier et al., 2000). The availability of satellite ocean-color imagery from the Sea-viewing Wide-Field of view Sensor (SeaWiFS) enables the assessment of these processes on regional to basin scales that cannot be achieved using point time series observations.

The present study considers the spring bloom in the central and western Sargasso Sea. Spring blooms in the Sargasso Sea have long been known to be driven by the seasonal input of new nutrients from winter mixing (Ryther and Menzel, 1960; Menzel and Ryther, 1961). Interannual variability in the magnitude of the spring bloom (i.e. total primary production and biomass) is generally attributed to interannual variability in the winter weather in the region (Menzel and Ryther, 1961). New production during the spring bloom is thought to represent 50% or more of the total annual new production for this region (Jenkins and Goldman, 1985; Michaels et al., 1994; Doney et al., 1996; Siegel et al., 1999). However, these new production estimates were derived from point time series in the vicinity of Bermuda Atlantic Time series Study station (BATS; Michaels and Knap, 1996; Steinberg et al., 2001). The extrapolation of these inferences to the region scale requires understanding of spatial variability and the nature of the processes regulating these fluxes (Siegel et al., 1990, 1999, 2002; Nelson et al., 2001).

Ocean-color imagery from the early Coastal Zone Color Scanner (CZCS) mission (McClain et al., 1990; Yoder et al., 1993) suggest that the springtime Sargasso Sea is characterized by smooth meridional gradients in chlorophyll and primary productivity. On the other hand, studies of mesoscale variability from field data and modeling (McGillicuddy et al., 1999), moored observations (Dickey et al., 1993, 2001; Wiggert et al., 1994), satellite altimetry (Siegel et al., 1999), and satellite ocean-color and sea-surface temperature (SST) observations (McGillicuddy et al., 2001) have indicated the presence of ubiquitous mesoscale physical features and short time course temporal changes that impact biogeochemical processes. These results clearly show that smooth

spatial gradients of long-term average quantities for the Sargasso Sea are the result of averaging over many short time-scale processes. Hence, the mean field picture will not be useful in diagnosing the mixing events that bring nutrients to the surface in the spring bloom, which occurs over short time and small spatial scales. This will correspondingly lead to underestimates in new production. Using remote sensing techniques that resolve the relevant time and space scales may help to alleviate this problem (Siegel et al., 1999).

A recent proxy-based analysis of the CO₂ sink in the Sargasso Sea (Nelson et al., 2001) showed that interannual differences in spatial meridional gradients of surface ocean processes were large even though interannual differences in net air–sea exchange of CO₂ at BATS were small. It was suggested that the differences in the meridional gradients of net CO₂ flux were driven by the regional extent of the spring bloom as controlled by winter mixing (Nelson et al., 2001). The purpose of this study is to test the hypothesis that meridional gradients in new production are driven by the extent of the spring bloom by applying proxy techniques for estimating new production to high-resolution (ca. 1 km) satellite data for the central Sargasso Sea region for four spring bloom seasons, 1997–2000. Proxy techniques for estimating new production have been based on phenomenological relationships between temperature and nutrients (e.g., Kamykowski and Zentara, 1986), but expressions incorporating the *f*-ratio (of new productivity to total productivity) and parameters of the photosynthesis–irradiance curve also have been used (Platt and Harrison, 1985; Platt et al., 1992). In the present study we have elected to consider only new production due to mixing-driven nitrate and nitrite input and are not estimating total productivity.

High-resolution satellite data are utilized for the present study for two reasons. First, these data best enable mesoscale patterns of variability to be taken into account. Second, high-resolution, direct-broadcast satellite data allow for the highest temporal resolution to be achieved, maximizing the number of cloud-free pixels (e.g. Campbell et al., 1995). The 16-fold greater data density and wider sampling swath afforded by local area

coverage (LAC) sampling compared with the global area coverage (GAC) data used to generate global products, increases the probability of coverage in both space and time. This approach also has allowed us to use three-day composite images rather than (for example) the eight-day composites used in SeaWiFS Standard Mapped Images (SMI, Campbell et al., 1995). This is hoped to provide our best opportunity to resolve short-term mixing events that we hypothesize are critical in driving the spring bloom of the Sargasso Sea. This approach takes full advantage of the capabilities of satellite data in conjunction with the high quality in situ data collected by the BATS program (Nelson et al., 2001; Steinberg et al., 2001; Siegel et al., 2001).

2. Methods

2.1. Study area

The area of the Sargasso Sea considered in the present study ($> 600,000 \text{ km}^2$) is outlined in Fig. 1. This area was selected primarily because of the high-resolution coverage afforded by SeaWiFS and AVHRR data received at the ground station in Bermuda. The BATS time-series site is also located close to the center of the study area,

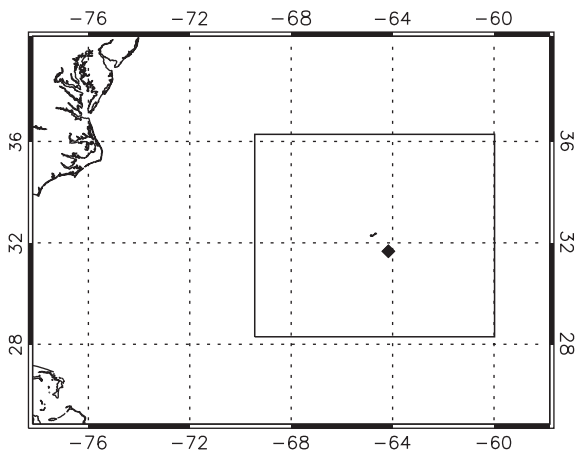


Fig. 1. The west central Sargasso Sea area covered by the present study (outline). The diamond symbol indicates the location of the BATS site ($31^{\circ}40'N$, $64^{\circ}10'W$) 80 km SE of Bermuda.

providing background and validation data. This region also was chosen to avoid the influence of the Gulf Stream, although Gulf Stream meanders or rings apparently influenced the northwest corner of the region during the time of the study (see Results). With the assumption that mean zonal gradients in surface properties of the Sargasso Sea are small (Nelson et al., 2001), we consider this region to be representative of the Sargasso Sea as a whole.

2.2. Nitrate index

We developed a proxy method for estimating the influx of new nitrate to surface waters during winter and spring mixing events (Lee et al., 2000; Goes et al., 1999, 2000). The method uses available SST imagery and assumes that the relationship between nitrate (+ nitrite) concentration and temperature developed from BATS data is constant (Fig. 2). Estimates of nitrate concentration calculated in this way are referred to as a “nitrate index” to emphasize the qualitative nature of this proxy. The central assumption of the proxy method is that cooler temperatures at the surface reflect deeper mixing, and thus greater influx of nitrogen to the surface. We have restricted our

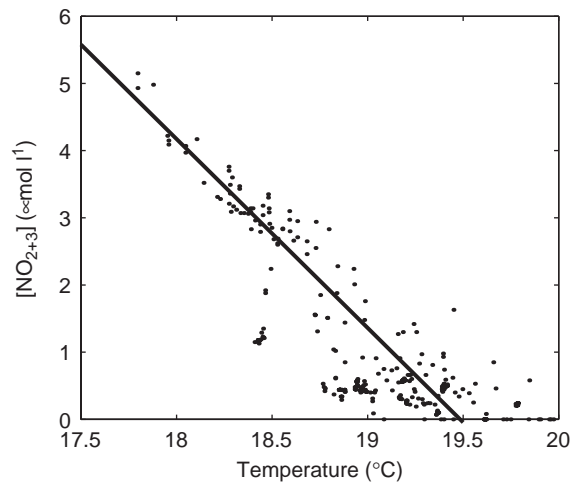


Fig. 2. Scatter plot of in situ temperature ($^{\circ}C$) vs. nitrate (+ nitrite) concentration ($\mu\text{mol l}^{-1}$) in samples collected at the BATS site, December–May. The solid line shows the result of the LAD regression done on the selected data (see Methods).

analysis to this relatively small area because of the completeness of the high-resolution satellite coverage, and to minimize the problem of assuming one temperature–nitrate relationship for the entire basin. World Ocean Atlas 1998 (Antonov et al., 1998) analysis data for a meridional transect across the study region (Fig. 1) at the BATS longitude suggest a <10% variation in the linear $T:\text{NO}_3$ relationship.

The temperature–nitrate relationship was derived from 242 BATS observations for the months of December–April (1994–2000) for depths from the surface down to the approximate depth of the subtropical mode water (ca. 300 m). From inspection of the data (Fig. 2), we estimated the nitrate depletion temperature to be ca. 20 °C and excluded data where the temperature was higher. The slope of the relationship was then found by minimizing the least average deviation (LAD regression, Dodge, 1997), rather than the usual least-squares method, in order to provide less weight to the outliers in the warmer near-surface samples (where phytoplankton activity may have already reduced nitrate concentration at the time of sampling). This regression resulted in the following relationship:

$$\text{NO}_{2+3} = \begin{cases} 54.77 - 2.811T, & T < 19.5^\circ\text{C}, \\ 0, & T \geq 19.5^\circ\text{C}, \end{cases} \quad (1)$$

where NO_{2+3} is the nitrate index (in units of $\mu\text{mol l}^{-1}$) and T is the temperature in degrees Celsius. This fit results in a nitrate depletion temperature of 19.5 °C with a linear correlation coefficient (R^2) of 0.71 and a root mean square (RMS) difference between model and data of $0.78 \mu\text{mol l}^{-1}$.

2.3. SST and nitrate index from AVHRR imagery

Sea-surface temperature was estimated from high-resolution (1.1 km at nadir) advanced very high resolution radiometer (AVHRR) imagery received by direct readout at the ground station in Bermuda (Nelson, 1998). Three-day composites of multichannel sea-surface temperature (MCSST) images (McClain et al., 1985) covering the study area (Fig. 1) were prepared according to the procedures described by Nelson (1998) and Nelson et al. (2001). Composite SST images agree well

with BATS temperature observations from the upper 2 m of the water column, with an RMS error of less than 0.5 °C (Nelson et al., 2001).

Nitrate index images corresponding to each SST composite image were prepared by applying the derived nitrate–SST relationship (Eq. (1)). Patches of elevated nitrate index are found north of the BATS site with spatial scales of 10's to several 100 km and concentrations reaching $1 \mu\text{mol l}^{-1}$.

High-resolution SST imagery for the spring bloom seasons of 1997, 1998, and 1999 are used here. The Bermuda receiving station failed during the spring of 2000 and lower-resolution global SST data (ca. 9 km; Brown et al., 1993) were used. Sufficient SeaWiFS HRPT imagery were available from nearby ground stations.

2.4. Chlorophyll *a* concentration and euphotic zone depth from SeaWiFS imagery

Chlorophyll concentrations at the surface were estimated from SeaWiFS HRPT imagery, collected from the Bermuda and NASA Goddard Spaceflight Center (GSFC) direct readout ground stations, and OCTS intensive local area coverage (I-LAC) data collected at the NASA Wallops Flight Facility and processed at GSFC. The resultant chlorophyll images were registered to the same projection as the AVHRR data as described above. Direct matches between SeaWiFS chlorophyll retrievals and measurements made at the BATS site are rare, but what validation data are present suggest that the SeaWiFS algorithm estimates chlorophyll concentration in the Sargasso Sea to within 50% of the field observed value ($n = 10$, $R^2 = 0.81$, RMS difference 0.065 mg m^{-3} at a mean value of ca. 0.125 mg m^{-3}). This is close to the SeaWiFS mission objectives of 35% RMS accuracy for chlorophyll pigment concentration (Hooker and McClain, 2000).

Euphotic zone depth for each composite image was determined by applying a power law parameterization developed by Siegel et al. (2001) relating in situ chlorophyll *a* concentration to the 1% of surface PAR depth

$$z_{\text{eu}} = 70.6(\text{Chl})^{-0.098}, \quad (2)$$

where z_{eu} is the euphotic zone depth (m) and (Chl) is the SeaWiFS-derived surface chlorophyll a concentration. This relationship assumes that the study area is within the same bio-optical province as the BATS site. The statistics for this estimate of the euphotic zone depth are poor ($R^2 = 0.31$), as more factors than chlorophyll significantly alter the euphotic zone depth (Siegel et al., 1995, 2001). Differences in average springtime new production estimates using the Siegel et al. (2001) formulation (Eq. (2)) and the Morel (1988) formulation were less than 5%.

2.5. Spring bloom new production estimates

New production driven by nitrate input is estimated by assuming that the nitrate index quantitatively reflects the nitrate concentration

throughout the euphotic zone and that changes in the nitrate index over short periods reflect input of nitrate from mixing and consumption of nitrate by phytoplankton. Thus the column new production rate ($\mu\text{mol N m}^{-2} \text{d}^{-1}$) is estimated as the *increase* in nitrate index per unit time for each nitrate influx event ($\mu\text{mol N m}^{-3} \text{d}^{-1}$) multiplied by the euphotic zone depth (m). Analogous methods have been used to estimate new production in the North Pacific (Goes et al., 1999, 2000) and in the vicinity of Bermuda using hydrographic data (Glover and Brewer, 1988; Siegel et al., 1990, 1999; Michaels et al., 1994). This method is applied to the study area (Fig. 1) by using composite SST images (e.g., Fig. 3A) to estimate the nitrate index (Fig. 3C) and SeaWiFS chlorophyll images (Fig. 3B) to estimate the euphotic zone depth. The cumulative error in this procedure was estimated by adding or

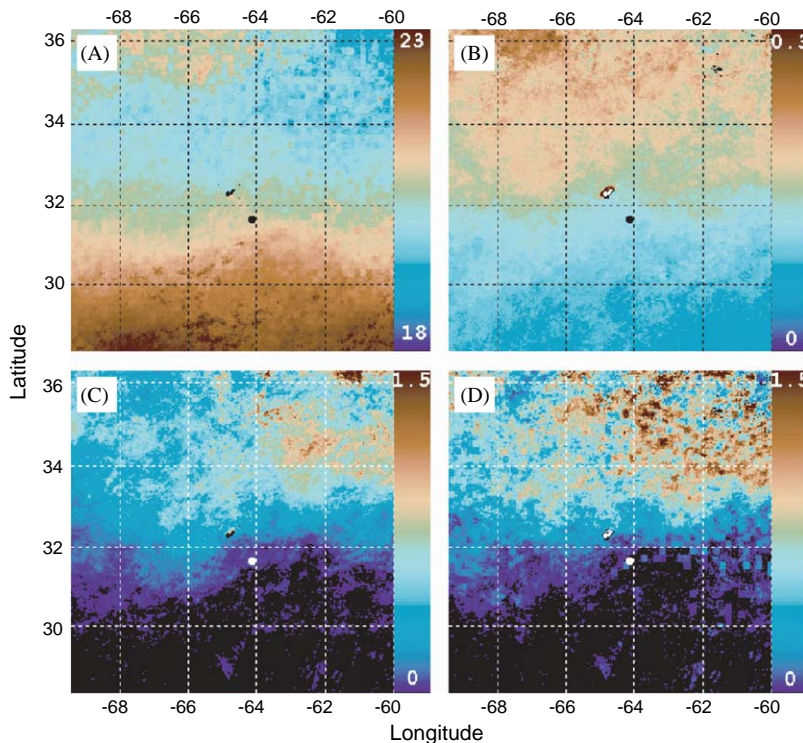


Fig. 3. Average springtime (December–June): (A) sea-surface temperature ($^{\circ}\text{C}$), (B) surface chlorophyll a concentration (mg m^{-3}), (C) nitrate index ($\mu\text{mol l}^{-1}$) and (D) new productivity ($\mu\text{mol N m}^{-2} \text{d}^{-1}$) for the period of the present study (December 1996–June 2000). Bermuda is shown at the center of the image (in white on panels A and C, black on panels B and D), and the BATS site is denoted by the dot (in black on panels A and B, and white on panels C and D). Black areas in (C) and (D) represent zero nitrate index values and zero new productivity values.

subtracting the RMS error for each of the input variables (SST and chlorophyll retrieval from satellite data) and the RMS error of the temperature vs. nitrate relationship to the nominal values. The resulting overestimates or underestimates of new productivity were compared to the nominal values. Average overestimate errors for each of the spring bloom seasons ranged from 30% to 46%. Underestimates tended to have smaller estimated error as the procedure does not allow the nitrate index (and thus estimated new production) to go below zero.

3. Results

3.1. Overall spatial distribution of surface ocean properties

Multi-year winter mean satellite-measured SST and chlorophyll *a* concentration, and the quantities we derived from them, are shown in Fig. 3. These images are arithmetic means of the three-day composite images for all data from the four spring bloom seasons (Jan–Jun). Average sea-surface temperature within the study region estimated from AVHRR data (Fig. 3A) ranged from 18 °C to 23 °C, with the BATS site located near the 21 °C isotherm. Within the individual images (not shown) the temperature range was from 15 °C to 25 °C. South of BATS little zonal variability is evident, but north of 35°N higher average temperatures are present west of 64°W due to the occasional passage of the Gulf Stream through the northwest part of the study area. In the vicinity of BATS, a region of warmer temperature extending northward is apparent between 62°W and 66°W. This feature is mirrored in the mean springtime chlorophyll *a* distribution (Fig. 3B), where chlorophyll concentrations are lower in the vicinity of BATS and Bermuda than elsewhere at the same latitude. Mean springtime chlorophyll concentrations within the study area range from 0.05 mg m⁻³ to near 0.3 mg m⁻³. As with the sea-surface temperature, little zonal variability is apparent south of BATS, but north of 35°N the chlorophyll concentrations and temperatures are higher west of 66°W. The highest

concentrations of chlorophyll were found in the northwest corner of the study area, possibly due to Gulf Stream rings or meanders in the area, which are much less likely to influence the north-east (Fig. 3B).

The maximum average values of the nitrate index derived from sea-surface temperature (Fig. 3C) were 1.5 μmol l⁻¹ north of 34°N and east of 64°W, where within individual images (not shown) the values were as high as 3 μmol l⁻¹. South of the BATS latitude (east of 64°W) and south of 30°N (west of 66°W), the nitrate index is non-zero only in patches. The average spatial distribution of springtime new productivity inferred from changes in the nitrate index and euphotic zone depth estimated from the chlorophyll images (Fig. 3D) resembles the average nitrate index distribution, with only patches of new productivity occurring south of the BATS latitude.

3.2. Meridional evolution of sea surface temperature and nitrate index

Meridional variations of the nitrate index are shown for the spring bloom seasons of 1996–1997 through 1999–2000 in Fig. 4. In this figure (and Figs. 5 and 6), the individual composite images have been zonally averaged, and the averages laid side by side to make a two-dimensional plot in order to show changes over time. The general pattern in each year is the emergence of elevated nitrate north of approximately 32°N after the first of the year. Values of the nitrate index are often as large as 3 μmol l⁻¹. As expected, large differences are observed among the four different years and the new nitrate inputs occur earlier in the year north of the BATS latitude (32°N). During 1997, nitrate index increased from 33°N to 36°N in late January (Fig. 5A). For the 1998 spring bloom, new nitrate inputs are smaller and patchy in character. However, this year shows the highest nitrate index values at the BATS latitude. The 2000 spring bloom had a large increase in nitrate concentrations (north of 33°N) and nitrate increased to a maximum of nearly 3 μmol l⁻¹ in late March (Fig. 4). The 1999 spring bloom had considerably lower nitrate index in its surface waters, and this pattern

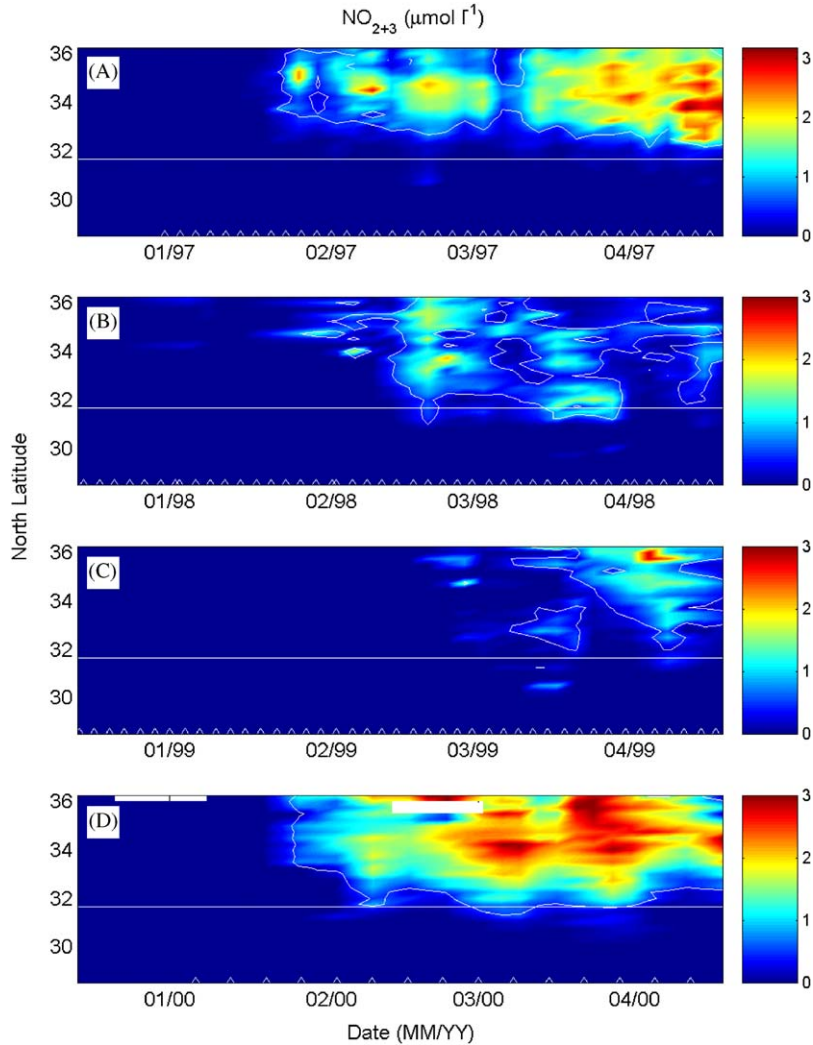


Fig. 4. Time-series of zonal averages of the nitrate index ($\mu\text{mol l}^{-1}$) derived from composite SST images. (A) 1996–1997. (B) 1997–1998. (C) 1998–1999. (D) 1999–2000. The white line shows the latitude of the BATS site, and the triangles at the bottom show the center dates of the composite images.

appeared to hold for all latitudes within the study area.

Zonal changes of inferred nitrate concentrations did not show consistent large scale patterns, and increases in new nitrate concentration occurred across the entire 60–69°W area in synchrony with the meridional increases (not shown). This pattern was consistent within each spring bloom season, indicating that the timing and extent of spring mixing events is mostly meridional. The zonal

differences in the average nitrate index distribution (Fig. 3C) are primarily driven by slight zonal gradients found primarily in the north of the study area.

3.3. Meridional distribution of phytoplankton pigment biomass

Meridional patterns of chlorophyll pigment concentration are poorly correlated to those found

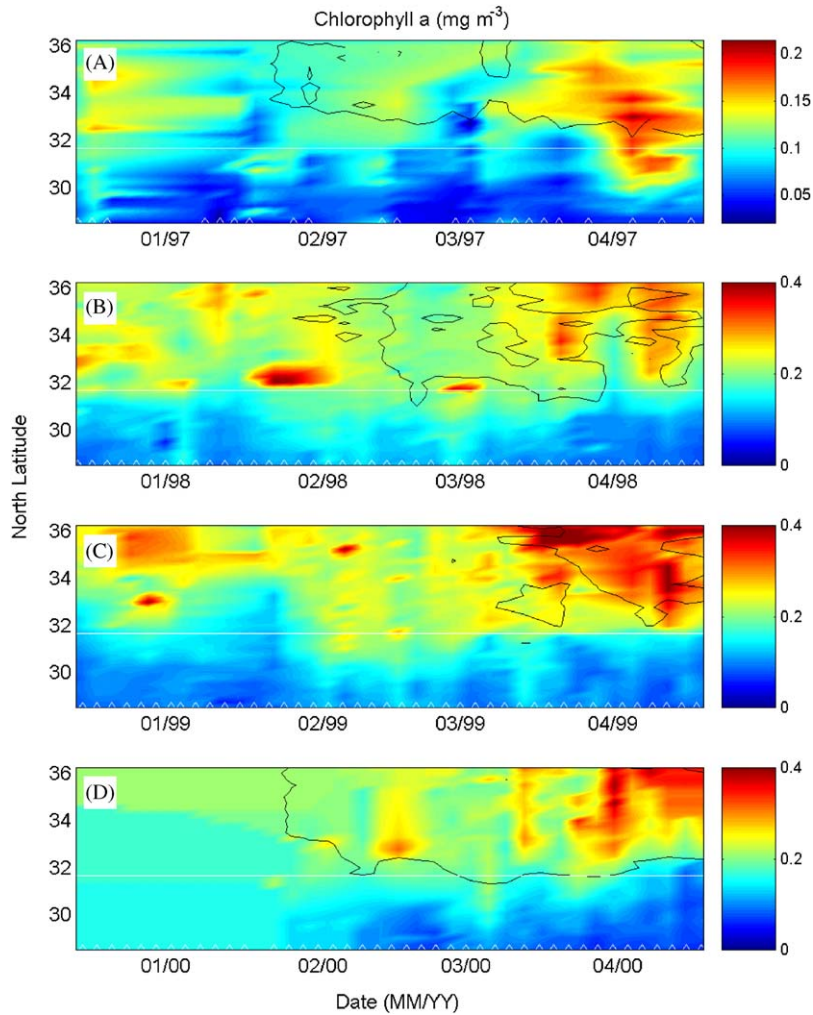


Fig. 5. Time-series of zonal averages of the chlorophyll a concentration (mg m^{-3}) derived from the three-day composite ocean-color images (A) 1996–1997 (B) 1997–1998 (C) 1998–1999 (D) 1999–2000. The white line shows the latitude or longitude of the BATS site. The black contour follows the 19.5°C nitrate depletion temperature. Triangles indicate the center dates of the composite images.

for nitrate index (Figs. 4 and 5). Linear correlation coefficients between nitrate and chlorophyll from the zonally averaged data were 0.09, 0.01, 0.06 and 0.03 for the four spring bloom seasons considered. On the other hand, the majority of pigment biomass accumulation appears to occur during the same time period as nitrate input. In particular, the highest chlorophyll concentrations occur where the SST is lower than 19.5°C , the nitrate depletion temperature (the black contours in Fig. 5). Clearly, this correspondence is far from perfect.

Zonal variability of the chlorophyll distribution (not shown) is again smaller than meridional variability, with some patchiness.

With some exceptions meridional gradients of chlorophyll concentration were positive (increasing with increasing latitude) throughout the region and were greatest during the spring bloom season (December–May of each year). Further, the largest meridional gradients occurred near the latitude of the BATS site and between 34°N and 36°N in 1998, 1999, and 2000. Chlorophyll a

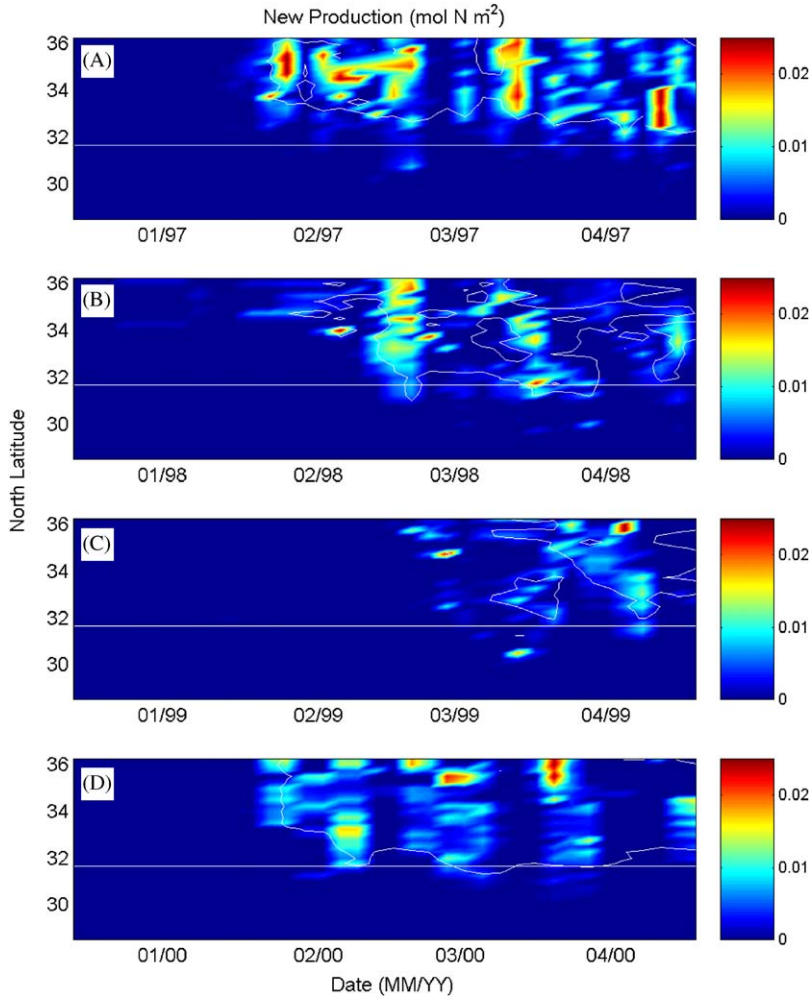


Fig. 6. Time-series of zonal averages of new production (mol N m^{-2}) derived from the three-day composite SST images (A) 1996–1997 (B) 1997–1998 (C) 1998–1999 (D) 1999–2000. The horizontal white line shows the latitude or longitude of the BATS site, and the white contour shows the 19.5°C isotherm.

concentrations estimated in 1996 and 1997 using the OCTS sensor (Fig. 5A) were significantly (factor of two) lower than those estimated in more recent years using the SeaWiFS sensor. The OCTS data was comparable to BATS in situ surface chlorophyll a concentration ($n = 3$, $R^2 = 0.76$, $\text{RMS difference} = 0.04 \text{ mg m}^{-3}$), so the reason for the lower OCTS chlorophyll composite values is not immediately obvious. On the other hand, temporal coverage of the study area with high-resolution data (I-LAC) was sparse compared to SeaWiFS HRPT coverage from the Bermuda

and GSFC ground stations (triangle symbols in Fig. 5 show the dates of three-day composites prepared). We are therefore forced to conclude that the 1997 spring bloom chlorophyll data are biased due to sparse temporal coverage, and the computed mean is lower than the actual. Because of the non-linear nature of Eq. (2), estimates of new production derived from these data may be ca. 10% higher due to the enhanced euphotic zone depth and the spatial distribution of new production rates may not be accurately represented.

3.4. Spatial patterns of new production estimates

Spatial/temporal patterns of new production estimated from the nitrate index and euphotic zone depth determinations (Fig. 6) are to first order similar to the nitrate index patterns (Fig. 4), only patchier as decreases in the nitrate index result in zero values of new production. The highest new production within the study area occurred in 1997, and the lowest in 1999. In 1997 and 2000 (Figs. 6A and D) significant new production was only found north of 32°N, but in the other years, significant patches of new productivity occurred at or south of the BATS latitude (Figs. 6B and C). These new production patches are ~200 km across and persist for about two weeks.

4. Discussion

4.1. Patterns of nitrate index and phytoplankton biomass

One interesting result of the present study was the lack of close correlation between zonal mean estimates of phytoplankton biomass (as estimated from satellite-derived chlorophyll, Fig. 5) and the nitrate index (Fig. 4). This is to be expected, as phytoplankton biomass is an estimate of stock, rather than a rate process, but it is customary to look at these processes as being correlated on the ocean-basin spatial scale and seasonal time scale rather than the 1 km and three-day time scale addressed in the present study (Siegel et al., 2001). In general terms the patterns of nitrate index and chlorophyll concentration are similar (largest values in March and April in the northern half of the region), but there is no significant correlation between the satellite data sets on the three-day time scale. This result indicates that similar disconnections between (for example) sediment trap flux, primary productivity, and biomass found in the field are not simply explained by unaccounted-for spatial and temporal variability on the mesoscale (e.g., Wiggert et al., 1994). On the time scale we are using in the present study, it is more likely that the phytoplankton biomass (as chlorophyll retrieved from ocean color) reflects

processes such as seasonal succession of phytoplankton populations (Steinberg et al., 2001), which occur on a longer time scale than the short-term mixing events we observe in the temperature imagery.

Interannual changes in nitrate index should correspond to large year-to-year differences in winter weather conditions and winter mixing (Menzel and Ryther, 1961; Michaels and Knap, 1996). These differences are thought to drive interannual differences in the strength and duration of the spring bloom conditions throughout the basin. Previous work has related the state of several climate oscillators to the intensity of winter mixing off Bermuda. For example, Michaels and Knap (1996) suggest that years of anomalously deep mixed-layer depths correspond to El Niño/Southern Oscillation (ENSO) events. Bates (2001) found that deep winter mixed layers correspond to periods when the North Atlantic Oscillation (NAO) is in its cool phase. For the period covered by the present study, the spring of 1998 corresponds to a strong El Niño event whereas the NAO was negative in 1997 and positive in the other years. Our present results are consistent with these hypotheses in the sense that the nitrate index was lowest within the study area during the 1999 spring bloom, when NAO was positive and there was no strong El Niño event.

4.2. Proxy estimates of new production in the central Sargasso Sea

We evaluated the effectiveness of the nitrate index proxy method for retrieving springtime new production by comparing our results for the BATS latitude with previous estimates made for the BATS location in particular (Table 1). Our results for 1998–2000 are comparable to the previous results, except for the 1992 results of Lipschultz (2001) based on ¹⁵N-nitrate uptake. This result is understandable, as some of the other studies cited in Table 1 used essentially the same method for estimating new production (i.e. BATS temperature vs. nitrate relationships). But this result also allows us to assume that our present proxy method is comparable to (or at least has the same limitations as) most other methods, and extend the results to

Table 1

Estimates of new production during the spring bloom at the BATS location (mol N m^{-2}) derived from the nitrate index and euphotic zone depth estimated from remote sensing data, compared with literature values derived using different methodology

Study	Convective flux (mol N m^{-2})	Method
Present study (1997)	0.074	Zonal average at BATS latitude (60–69 W) using nitrate index from satellite SST and euphotic zone depth from satellite chlorophyll <i>a</i>
Present study (1998)	0.227	
Present study (1999)	0.055	
Present study (2000)	0.137	
Present study mean (std. dev.)	0.123 (0.08)	
Siegel et al. (1999)	0.17 (0.05)	BATS hydrography (1989–1995)
Mean (std. dev.)	Range 0.06–0.23	
Doney et al. (1996)	0.24	Ecosystem model
Michaels et al. (1994)	0.17	BATS hydrography (1989–1993)
Glover and Brewer (1988)	0.30	Climatology of MLD and NO_3
Lipschultz (2001)	0.87, 0.10	^{15}N incubation (1992, 1993)

Table 2

Proxy estimates of mean areal springtime new production (mol N m^{-2}) for the central Sargasso Sea (Fig. 1) compared to a similar proxy estimate for the BATS latitude alone, based upon integrals of time-and-space variable new production (December–June, Fig. 7)

Year	NP at BATS	Regional NP	Ratio
1996–1997	0.074	0.303	0.25
1997–1998	0.227	0.174	1.30
1998–1999	0.055	0.090	0.61
1999–2000	0.137	0.197	0.70
Mean (S.D.)	0.12 (0.078)	0.19 (0.088)	0.71 (0.44)

at least the local region (Fig. 1). The high new production found in 1992 by Lipschultz (2001) is well outside the range of new production found in the other studies (Table 1), but his 1993 results were within the range found in the present study and the others reported in 2001.

Accepting the assumption that the temperature–nitrate relationship for BATS holds throughout the region outlined in Fig. 1, we can test the hypothesis that springtime new production at the BATS site reflects the entire region. We compared the proxy estimate of springtime new production for the BATS site to the integral of the entire region (Table 2), and found no relationship between the two ($R^2 = -0.01$). The reason for this disagreement is apparent after inspecting Figs. 5–7. The total springtime new production

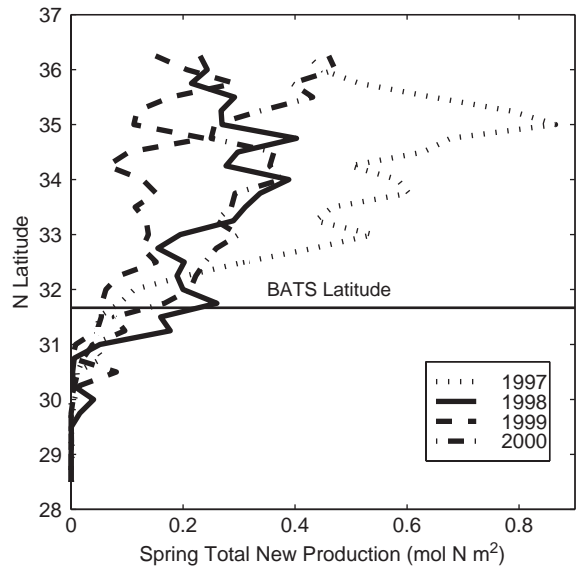


Fig. 7. Summary of total zonally averaged new production (mol N m^{-2}) vs. latitude across the west central Sargasso Sea region (highlighted area in Fig. 1) estimated from SST and ocean-color imagery, for the 1997–2000 spring bloom seasons.

at BATS as estimated from the proxy method is very strongly dependent upon the meridional gradient of sea-surface temperature and thus the nitrate index. In years when the 19.5°C contour extends below the latitude of BATS, the local new production is high, but this may or may not reflect regional high production and vice versa.

In 1996–1997, the nitrate index was high from January–June continuously north of the BATS site, but this high nitrate index region did not extend to the BATS latitude. Conversely, in 1997–1998, the regional new production was lower and had a later onset, but new production at BATS was higher than in 1997 due to a shallower meridional gradient. In 1999 and 2000, relative new production at BATS was consistent with relative new production throughout the region. This assessment holds true even if our less-confident estimate of new production in 1996–1997 is excluded. Therefore, springtime new production at BATS is not a good predictor of springtime new production across the entire Sargasso Sea.

4.3. Spatial gradients of sea surface properties and implications for new production

It is evident that springtime new production within the region outlined in Fig. 1 and as estimated by our proxy method is controlled on an annual basis by the timing of the onset of convective mixing, and by the meridional gradient of mixing. At the BATS site, this meridional gradient seems to be more important in determining whether significant mixing and therefore new production occurs. South of BATS springtime new production declines to \sim zero near 30°N (Fig. 7). For the small region we consider in the present work zonal gradients are not significant; however, Nelson et al. (2001) found some zonal trends in SST-derived $p\text{CO}_2$ in the eastern Sargasso Sea, so their importance within regions larger than the present study area (Fig. 1) should not be ruled out. Significant zonal gradients in SST were found during the frontal air-sea interaction experiment (FASINEX) study to the south of the present study area (Halliwell and Cornillon, 1990; Halliwell et al., 1991).

The proxy spring new production at BATS was well correlated with the total new production in the region in 1999–2000 but not in 1996–1997 or 1997–1998. This result suggests the presence of a frontal region, which is sometimes north and sometimes south of BATS, which determines the southward extent of winter mixing. In each year

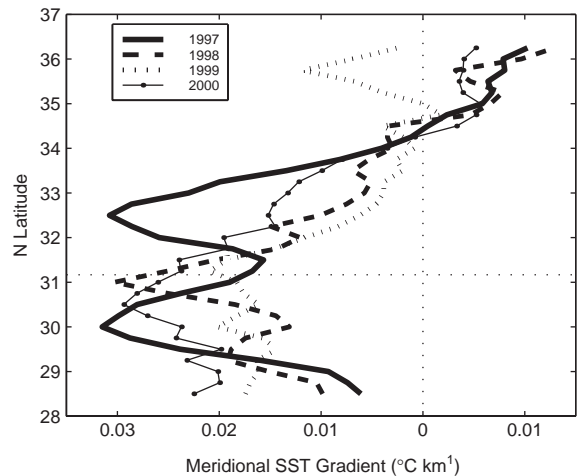


Fig. 8. Meridional gradients of sea-surface temperature ($^\circ\text{C km}^{-1}$) vs. latitude, average value for the spring season (December–June), for each of the years considered in the present study. The dotted line shows the latitude of the BATS station.

the largest meridional gradient in sea-surface temperature (as much as $-0.03^\circ\text{C km}^{-1}$) was found throughout the spring season in a region between 30° and 33°N (Fig. 8). North and south of this zonal band, SST gradients were much closer to zero (and are in fact slightly positive at the north edge of the study region, which approaches the Gulf Stream). This meridional gradient feature persists from year to year despite differences in the local SST (Fig. 8). We suggest that this feature represents a distinct physical boundary between the seasonally mixed northern Sargasso Sea and the permanently stratified southern Sargasso Sea (Menzel and Ryther, 1961; Siegel et al., 1990). In this context it is easy to see how the BATS site may be sensitive to changes in the local area, which may or may not reflect the overall new productivity of the region.

5. Conclusions

In the present study we have applied BATS nutrient and hydrographic data in conjunction with remote-sensing proxy-derived quantities to estimate springtime new production in a $> 600,000 \text{ km}^2$ region of the central Sargasso Sea

surrounding the BATS site for the years 1997–2000. Interannual variability was significant, and was probably due to the influence of ENSO and NAO-driven changes in climatological forcing. We found little correlation between phytoplankton biomass (as ocean-color-derived chlorophyll) and new production rates, and little correlation between the annual totals of new production at BATS and integrated within the entire region.

We attribute the lack of correlation between BATS new production and regional new production to the fact that the latitude of BATS was at the center of a meridional sea surface temperature front region. Significant changes in nutrient supply at the BATS site resulted from small changes in the position of the front from year to year that were not always correlated with basin-scale processes. These results continue to highlight the importance of regional data in conjunction with the time-series sites in order to place their results in the appropriate context.

Acknowledgments

This research was supported by the NASA Earth Science Enterprise, Ocean Biology and Biogeochemistry Program. SeaWiFS data courtesy of the SeaWiFS Project, NASA Goddard Spaceflight Center, and Orbimage. OCTS I-LAC data courtesy of NASDA and GSFC. AVHRR mcst data not acquired at Bermuda were obtained from the JPL Physical Oceanography DAAC. Thanks to Manuela Lorenzi-Kayser, Maureen Keneally, Margaret O'Brien, Ru Morrison and Alec Scott, for technical assistance. BATS project data from the Bermuda Biological Station for Research, funded by the NSF Division of Ocean Sciences.

References

- Antonov, J.I., et al., 1998. World Ocean Atlas 1998. US Department of Commerce, National Oceanic and Atmospheric Administration, National Environmental Satellite, Data, and Information Service; Silver Spring, MD. (National Oceanographic Data Center, User Services Branch, distributor)
- Bates, N.R., 2001. Interannual variability of oceanic CO₂ and biogeochemical properties in the Western North Atlantic subtropical gyre. *Deep-Sea Research II* 48, 1507–1528.
- Brown, J.W., Brown, O.B., Evans, R.H., 1993. Calibration of advanced very high resolution radiometer infrared channels: a new approach to nonlinear correction. *Journal of Geophysical Research* 98, 18257–18268.
- Campbell, J.W., Blaisdell, J.M., Darzi, M., 1995. Level-3 SeaWiFS data products: spatial and temporal binning algorithms. In: Hooker, S.B., Firestone, E.R., Acker, J.G. (Eds.), *SeaWiFS Technical Report Series*, Vol. 32. NASA Tech. Memo. 104566.
- Dickey, T.D., Granata, T., Marra, J., Langdon, C., Hamilton, M., Wiggert, J., Chai-Jochner, Z., Hamilton, M., Vazquez, J., Stramska, M., Bidigare, R., Siegel, D., Bratkovich, A., 1993. Seasonal variability of bio-optical and physical properties in the Sargasso Sea. *Journal of Geophysical Research* 98, 865–898.
- Dickey, T.D., et al., 1998. Initial results from the Bermuda Testbed Mooring program. *Deep-Sea Research I* 45, 771–794.
- Dickey, T.D., et al., 2001. High temporal resolution measurements from the Bermuda Testbed Mooring: June 1994–March 1998. *Deep-Sea Research II* 48, 2105–2140.
- Dodge, Y., 1997. LAD regression for detecting outliers in response and explanatory variables. *Journal of Multivariate Analysis* 61, 144–158.
- Doney, S.C., Glover, D.M., Najjar, R.G., 1996. A new coupled, one-dimensional biological-physical model for the upper ocean—applications to the JGOFS Bermuda Atlantic Time-series Study (BATS) site. *Deep-Sea Research II* 43, 591–624.
- Glover, D.M., Brewer, P.G., 1988. Estimates of winter-time mixed layer nutrient concentrations in the North Atlantic. *Deep-Sea Research* 3, 1525–1546.
- Goes, J.I., Saino, T., Oaku, H., Ding, L.J., 1999. A method for estimating sea surface nitrate concentrations from remotely sensed SST and chlorophyll a—a case study for the North Pacific Ocean using OCTS/ADEOS data. *IEEE Transactions on Geosciences and Remote Sensing* 37, 1633–1644.
- Goes, J.I., Saino, T., Ishizaka, J., Wong, C.S., Nojiri, Y., 2000. Estimating sea surface nitrate from space by compound remote sensing. *Geophysical Research Letters* 27, 1263–1265.
- Halliwel, G.R., Cornillon, P., 1990. Large-scale SST variability in the western North Atlantic subtropical convergence zone during FASINEX. 1: Description of SST and wind stress fields. *Journal of Physical Oceanography* 20, 209–222.
- Halliwel, G.R., Cornillon, P., Brink, K.H., Pollard, R.T., Evans, D.L., Regier, L.A., Toole, J.M., Schmitt, R.W., 1991. Descriptive oceanography during the frontal air-sea interaction experiment: Medium- to large-scale variability. *Journal of Geophysical Research* 96, 8553–8567.
- Hooker, S.B., McClain, C.R., 2000. The calibration and validation of SeaWiFS data. *Progress in Oceanography* 45, 427–465.

- Jenkins, W.J., Goldman, J.C., 1985. Seasonal oxygen cycling and primary production in the Sargasso Sea. *Journal of Marine Research* 43, 465–491.
- Kamykowski, D., Zentara, S.J., 1986. Predicting plant nutrient concentrations from temperature and sigma-t in the upper kilometer of the world ocean. *Deep-Sea Research* 33, 89–105.
- Lipschultz, F., 2001. A time-series assessment of the nitrogen cycle at BATS. *Deep-Sea Research II* 48, 1897–1924.
- Longhurst, A.R., 1998. *Ecological Geography of the Sea*. Academic Press, San Diego.
- Lee, K., Wanninkhof, R., Feely, R.A., Millero, F.J., Peng, T.-H., 2000. Global relationships of total inorganic carbon with temperature and nitrate in surface seawater. *Global Biogeochemical Cycles* 14, 979–994.
- Letelier, R.M., Karl, D.M., Abbott, M.R., Flament, P., Freilich, M., Lukas, R., Strub, T., 2000. The role of late winter meso-scale events in the biogeochemical variability of the upper water column of the North Pacific Subtropical Gyre. *Journal of Geophysical Research* 105, 28,723–28,739.
- McClain, C.R., Esaias, W.E., Feldman, G.C., Elrod, J., Endres, D., Firestone, J., Darzi, M., Evans, R., Brown, J., 1990. Physical and biological processes in the North Atlantic during the first GARP global experiment. *Journal of Geophysical Research* 95, 18027–18048.
- McClain, E.P., Pichel, W.G., Walton, C.C., 1985. Comparative performance of AVHRR-based multichannel sea surface temperatures. *Journal of Geophysical Research* 90, 11587–11601.
- McGillicuddy, D.J., Johnson, R., Siegel, D.A., Michaels, A.F., Bates, N.R., Knap, A.H., 1999. Mesoscale variations of biogeochemical properties in the Sargasso Sea. *Journal of Geophysical Research* 104, 13381–13394.
- McGillicuddy Jr., D.J., Kosnyrev, V.K., Ryan, J.P., Yoder, J.A., 2001. Covariation of mesoscale ocean color and sea-surface temperature patterns in the Sargasso Sea. *Deep-Sea Research II* 48, 1823–1836.
- Menzel, D.W., Ryther, J.H., 1961. Annual variations in primary production of the Sargasso Sea off Bermuda. *Deep-Sea Research* 7, 282–288.
- Michaels, A.F., Knap, A.H., 1996. An overview of the US JGOFS Bermuda Atlantic Time-series Study and the Hydrostation S program. *Deep-Sea Research II* 43, 157–198.
- Michaels, A.F., et al., 1994. Seasonal patterns of ocean biogeochemistry at the US JGOFS Bermuda Atlantic Time-series Study site. *Deep-Sea Research* 41, 1013–1038.
- Morel, A., 1988. Optical modeling of the upper ocean in relation to its biogenous matter content case I waters. *Journal of Geophysical Research* 93, 10749–10768.
- Nelson, N.B., 1998. Spatial and temporal extent of sea surface temperature modifications by hurricanes in the Sargasso Sea during the 1995 season. *Monthly Weather Review* 126, 1364–1368.
- Nelson, N.B., Bates, N.R., Siegel, D.A., Michaels, A.F., 2001. Spatial variability of the CO₂ sink in the Sargasso Sea. *Deep-Sea Research II* 48, 1801–1822.
- Platt, T., Harrison, W.G., 1985. Biogenic fluxes of carbon and oxygen in the ocean. *Nature* 318, 55–58.
- Platt, T., Sathyendranath, S., Ulloa, O., Harrison, W.G., Hoepffner, N., Goes, J., 1992. Nutrient control of phytoplankton photosynthesis in the Western North Atlantic. *Nature* 356, 229–231.
- Ryther, J.H., Menzel, D.W., 1960. The seasonal and geographic range of primary production in the western Sargasso Sea. *Deep-Sea Research* 6, 235–238.
- Siegel, D.A., Iturriaga, R., Bidigare, R.R., Pak, H., Smith, R.C., Dickey, T.D., Marra, J., Baker, K.S., 1990. Meridional variations of the springtime phytoplankton community in the Sargasso Sea. *Journal of Marine Research* 48, 379–412.
- Siegel, D.A., Michaels, A.F., Sorensen, J.C., O'Brien, M., Hammer, M.A., 1995. Seasonal variability of light availability and utilization in the Sargasso Sea. *Journal of Geophysical Research* 100, 8675–8713.
- Siegel, D.A., McGillicuddy, D.J., Fields, E.A., 1999. Mesoscale eddies, satellite altimetry, and new production in the Sargasso Sea. *Journal of Geophysical Research* 104, 13359–13379.
- Siegel, D.A., Nelson, N.B., O'Brien, M.C., Westberry, T.K., Morrison, J.R., Michaels, A.F., Caporelli, E.A., Sorensen, J.C., Garver, S.A., Brody, E.A., Ubante, J., Hammer, M.A., 2001. The Bermuda Bio-Optics Project: bio-optical modeling of primary production from space-sensible variables. *Deep-Sea Research II* 48, 1865–1896.
- Siegel, D.A., Doney, S.C., Yoder, J.A., 2002. The spring bloom of phytoplankton in the North Atlantic ocean and Sverdrup's critical depth hypothesis. *Science* 296, 730–733.
- Steinberg, D.K., Carlson, C.A., Bates, N.R., Johnson, R.J., Michaels, A.F., Knap, A.H., 2001. Overview of the US JGOFS Bermuda Atlantic Time-series Study (BATS): a decade-scale look at ocean biology and biogeochemistry. *Deep-Sea Research II* 48, 1405–1448.
- Wiggert, J., Dickey, T., Granata, T., 1994. The effect of temporal undersampling on primary production estimates. *Journal of Geophysical Research* 99, 3361–3371.
- Yoder, J.A., McClain, C.R., Feldman, G.C., Esaias, W.E., 1993. Annual cycles of phytoplankton chlorophyll concentrations in the global ocean—a satellite view. *Global Biogeochemical Cycles* 7, 181–193.